RSC Advances

PAPER

View Article Online
View Journal | View Issue

Check for updates

Cite this: *RSC Adv.*, 2022, **12**, 9404

Establishing an energy-saving scouring/bleaching one-step process for cotton/spandex fabric using UVA-assisted irradiation†

Qing Li, [abc] Xiaowei Zhao,[d] Heng Quan*[a] and Yuyang Zhou *[c]

To reduce the energy and water consumption from a conventional textile industry, a facile and efficient UVA-assisted scouring/bleaching strategy has been customized for cotton/spandex in this research. The bleaching efficacy under UVA irradiation is explored by comparing diverse processes, *i.e.*, Scouring only (Sc.); Conventional scouring and pad-steam bleaching (Sc/$Bl_{Conv\text{-}PS}$); Conventional scouring and cold pad-batch bleaching (Sc/$Bl_{Conv\text{-}CPB}$); and one or two-step scouring and UVA-assisted bleaching (Sc/Bl_{UVA}-I, Sc/Bl_{UVA}-II). The significance, interactive effect and optimisation of parameters on the whiteness index (WI) of fabric are investigated through mathematical modelling. The bleaching mechanism is analysed by a fluorescence labelling method. The dyeing and tensile properties of fabrics and the energy conservation during processing are also demonstrated. Results show that Sc/Bl_{UVA}-I achieves an equivalent scouring and bleaching effect as Sc/Bl_{UVA}-II. A superior bleaching effect of Sc/Bl_{UVA}-II over that of Sc/Bl_{Conv}-PS reveals the better function of catalytic UVA than conventional steam. Under the theoretical optimal bleaching conditions (H_2O_2 conc. 42.96 g L^{-1}, pH 10.24 and irradiation time 3.68 h), a calculated highest WI of 77.19 (1.48 times higher than that of untreated fabric) can be achieved based on the mathematical modelling. Through mechanism studies, hydroxyl radicals are confirmed as the main oxidative species taking part in UVA-assisted bleaching and their concentration in simulated bleaching solution dramatically increases upon the introduction of UVA. The fabric treated by Sc/Bl_{UVA}-I exhibits an acceptable strength decrease (<10%) and excellent dyeing performance with reactive dyes. The Sc/Bl_{UVA}-I strategy enables more than *ca.* 70% of energy conservation than the Sc/$Bl_{Conv\text{-}PS}$ process. The encouraging results manifest the practicability and promising prospects of UVA-assisted pre-treatment which contributes to enhancing the sustainability of the textile industry.

Received 31st January 2022
Accepted 13th March 2022

DOI: 10.1039/d2ra00659f

rsc.li/rsc-advances

Open Access Article. Published on 25 3 2022. Downloaded on 2024/10/18 9:57:24.
This article is licensed under a Creative Commons Attribution-NonCommercial 3.0 Unported Licence.

1. Introduction

Conventional textile processing usually requires large water/energy consumption and effluent discharge, which puts it out of the scope of sustainable industry.[1–3] Bleaching is a necessary procedure especially for cellulosic fabric such as cotton, linen, viscose to remove intrinsic colored substances towards desirable whiteness for the subsequent dyeing and finishing process. Conventional bleaching is generally undertaken in large-volume water bath relying on the heavy consumption of hydrogen peroxide (H_2O_2), alkaline agent, and heat energy to elevate temperature up to 98 °C under continuous processing for 30–60 min, which not only leads to unexpected fibre damage but also aggravates the global carbon emission rising from energy generation.[4–6] Moreover, a diverse of pollutants including oxidant, alkali, silicate, surfactant generated from bleaching chemicals exert adversely impact on water quality leaving additional burden on wastewater treatment.[7,8] Therefore, to establish a water/energy saving bleaching process for cellulosic fabric is on a desperate demand from textile sector towards sustainable industry, which simultaneously tackles with the freshwater crisis and carbon emission - two globally most pressing issues at present.

To date, a diverse of novel chemicals and advanced techniques have been introduced to the bleaching system for textiles. Low-temperature bleach activators like *N*-[4-(triethylammoniomethyl)-benzoyl]-caprolactam-chloride (TBCC), sodium 4-(nonanoyloxy)benzene sulphonate (NOBS),

[a]*Hubei Key Laboratory of Biomass Fibers and Eco-Dyeing & Finishing, Wuhan Research Center of Eco-dyeing & Finishing and Functional Textile, College of Chemistry and Chemical Engineering, Wuhan Textile University, 1 Yangguang Avenue, Wuhan 430200, China. E-mail: quanheng2002@163.com*

[b]*Key Laboratory of Clean Dyeing and Finishing Technology of Zhejiang Province, Shaoxing University, Shaoxing, China*

[c]*Jiangsu Engineering Research Center of Textile Dyeing and Printing for Energy Conservation, Discharge Reduction and Cleaner Production, National Engineering Laboratory for Modern Silk, College of Textile and Clothing Engineering, Soochow University, 199 Renai Road, Suzhou 215123, China. E-mail: zhouyuyang_suda@hotmail.com*

[d]*Zhejiang Tengma Textile Co., Ltd., Chunlan Road, Lanxi 321100, China*

† Electronic supplementary information (ESI) available. See DOI: 10.1039/d2ra00659f

© 2022 The Author(s). Published by the Royal Society of Chemistry

Open Access Article. Published on 25 3 2022. Downloaded on 2024/10/18 9:57:24.
This article is licensed under a Creative Commons Attribution-NonCommercial 3.0 Unported Licence.

tetra-acetylethylenediamine (TAED), tetraacetyl hydrazine (TH) and glycerol triacetate (GT) have been widely studied for efficient bleaching in recent years.[5,9–12] Perhydrolysis reaction starts where peracid is formed by the nucleophilic reaction of perhydroxyl anions (HO_2^-) with the activators.[13] Although higher efficiency and lower temperature of bleaching are achieved, the introduction of bleach activators raises additional environmental concern. For example, TH and TBCC are not recommended due to their eco-toxicity according to a recent report.[14] Apart from chemicals, ozone, sonication, microwave, plasma techniques are also involved for efficient textile bleaching.[15–18] Our recent research confirms the dramatic enhancement of bleaching efficiency by integrating ultrasonic technology and a low-toxic bleaching activator – TAED.[19]

Nowadays, ultraviolet (UV)-assisted bleaching has been praised as a promising sustainable alternative to conventional process for its high efficiency, operational simplicity and safety, and cost effectiveness.[15] Significantly, both energy consumption (available for room-temperature implementation) and wastewater effluent are diminished due to the direct UV radiation on fabric rather than immersing fabric in a heated bleaching bath. Under UV radiation, the hydroxyl radicals (HO·) as a powerful oxidant generated from the homolytic cleavage of the O–O bond of H_2O_2,[20,21] enables fast breakage of double bonds in conjugated system of coloured impurities, thereby destroying the impurities responsible for yellowish appearance.[22,23] The major drawback of UV-assisted bleaching especially for short wavelength of UV (*e.g.* UVC at ~254 nm) irradiation, is related to the great strength loss of cotton fabrics for about 50% due to the high UVC energy that attacks the main cellulosic chain.[23,24] UVB locates at longer wavelength of ~312 nm, and displays a higher decolorising efficiency and strength retention of cotton fibre than H_2O_2/UVC bleaching system.[25] As yet, less recognition has been given to the application of low energy UVA (320–400 nm) for textile bleaching. UVA/H_2O_2 system has been confirmed as a successful and efficient strategy for oxidative degradation of dyes, micropollutants and antibiotics in wastewater based on the photocatalytic activity of UVA.[26–28] With these in mind, it is reasonable to design UVA-assisted H_2O_2 bleaching system to degrade colour impurities on cellulosic fabric probably with better fiber protection due to the low energy of UVA than those under UVB and UVC. Further, the bleaching feasibility, decolorization mechanism, and process optimisation of UVA/H_2O_2 system are also pending for in-depth exploration.

Cotton/spandex fabric that combines the hygroscopicity and comfortableness of cotton and stretchability of spandex, is a desirable textile material for jeans, apparel, hosiery, *etc.*[29,30] Spandex has a higher price than cotton, and merely with low addition (~3%) of which enables significant elastration of fabric. However, elastration drop of spandex easily occurs at high temperature, pH and oxidant concentration. Therefore, the challenge for the bleaching of cotton/spandex over pure cotton fabric is to achieve a desirable whiteness but with less mechanical sacrifice. Fortunately, UVA-assisted bleaching appears to be an appropriate option customised for cotton/spandex fabric. However, few studies have made attempts to verify such assumption. Therefore in the present research, a facile and efficient UVA-assisted H_2O_2 bleaching strategy is customized for cotton/spandex that simultaneously reduces the energy and water consumption. The bleaching efficacy of UVA-assisted bleaching was revealed through the comparison with the conventional process. To address the practical mass manufacturing needs, the significance, interactive effects and optimisation of variables (H_2O_2 concentration, pH value and irradiation time) on whiteness index (WI) of fabrics were explored by mathematical modelling through a central composite design (CCD) using Minitab 19 Software (Trial version). The bleaching mechanism stemmed from the catalytic effect of UVA on H_2O_2 dissociation, was demonstrated by fluorescence labelling method. The dyeing and tensile properties of cotton/spandex after bleaching were also examined. Finally, the energy conservation of UVA-assisted bleaching was estimated compared with that of conventional bleaching.

2. Material and method

2.1. Materials

Cotton/spandex fabric that contains 97% cotton/3% spandex with a density of 290 g m^{-2} (warp density: 148 ends per inch, weft density: 73 ends per inch), was provided by Zhejiang Tengma Textile Co., Ltd., China. Penetrating agent, *i.e.* surfactant 1303 (Industrial grade) is a non-ionic polyoxyethylene ether surfactant bought from Jiangsu Haian Petroleum Chemical Plant, China. Hydrogen peroxide (30%, w/w), sodium sulphate, sodium carbonate, sodium hydroxide, and dimethyl sulphoxide (DMSO) used are in analytical grade. Benzenepentacarboxylic acid (BA, purity > 98%) was purchased from TCI Chemical Industry Co. Ltd., China. Three reactive dyes named RED FN-2BL, YELLOW FN-2R and BLUE FN-R representing three distinctive colour hues, were bought from Huntsman Co., Ltd. Neutral detergent (Industrial grade) for the soaping of dyed fabric was obtained from Ningbo Runhe High-Tech Material Co., Ltd., China. All water used is deionized water. In addition, all the H_2O_2 mentioned refers to pure H_2O_2 thus no further emphasized is placed in the following text.

2.2. Fabric treatment

The experiment design is schematically described in Fig. 1. More details are provided in the following sections.

2.2.1. UVA-assisted H_2O_2 bleaching. Both two-step (scouring followed by bleaching) and one-step (simultaneous scouring and bleaching) methods were developed for contrastive study.

Two-step process. Ten gram of greige (Untr.) fabric (A) was scoured using 2 g L^{-1} surfactant 1303 at 95 °C for 10 min at a liquor ratio of 15 : 1, rinsed thoroughly with deionized hot water (50 °C) to remove residual surfactant, and dried for the following bleaching process. The obtained only scoured (Sc.) fabric (B) was the control sample used for contrastive analysis. For bleaching process, the fabric was subjected to a dip-pad process using a laboratory padding mangle (Xiamen Rapid, China) with bleaching solution and exposed to UVA lamps. The bleaching solution was formulated by 30 g L^{-1} H_2O_2 and 10 g

© 2022 The Author(s). Published by the Royal Society of Chemistry

Open Access Article. Published on 25 3 2022. Downloaded on 2024/10/18 9:57:24.
This article is licensed under a Creative Commons Attribution-NonCommercial 3.0 Unported Licence.

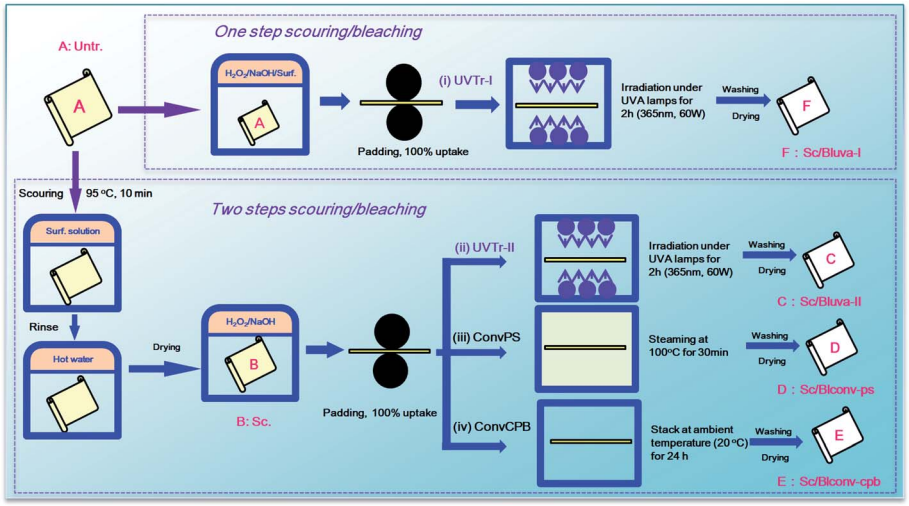

Fig. 1 Design of scouring and bleaching routines. Note: Untr.: untreated fabric; Sc.: only scoured fabric; Sc/Bl_{UVA}-I: one step scoured and UVA bleached fabric; Sc/Bl_{UVA}-II: two steps scoured and UVA bleached fabric; Sc/Bl_{conv}-ps: two steps scoured and conventional pad-steam bleached fabric; Sc/Bl_{conv}-cpb: Two steps scoured and conventional cold pad-batch bleached fabric; UVTr-I: UV treated-one step process; UVTr-II: UV treated-two steps process; ConvPS: Conventional pad-steam bleaching; ConvCPB: conventional cold pad-batch bleaching.

L^{-1} sodium hydroxide at pH 12.5, and loaded onto fabric through a dip-pad-dip-pad process with uptake ratio of 100% under roller pressure of 1 kg cm^{-2}. The dipping process was repeated twice and each for 2 min. To achieve a uniform UVA light exposure, a lamp-box installed with 6 UVA lamps was designed to enable its facing to fabric at a peak wavelength of 365 nm using a power of 15 W (Fig. S1†). The total irradiation power was adjusted to 30 W, 60 W or 90 W by lamp switch. According to the result of pre-experiment (Fig. S2†), 60 W was the suitable power considering the bleaching effectiveness and energy consumption. The fabric was exposed to UVA lamps (TLD 15W/03, Philips Co., Ltd.) from 20 cm away at 35 °C, flipped over every 30 min for 2 h, then thoroughly rinsed with deionized water, and dried in the open air. Such process and the resultant fabric are denoted as UVTr-II (ii) and Sc/Bl_{UVA}-II (C), respectively.

One-step process. The padding solution was formulated by 30 g L^{-1} H_2O_2, 10 g L^{-1} sodium hydroxide and 2 g L^{-1} surfactant 1303 at pH 12.5. The dip-pad-dip-pad and UV irradiation processes were the same as mentioned above. Such process and the resultant fabric are denoted as UVTr-II (i) and Sc/Bl_{UVA}-I (F), respectively.

2.2.2. Conventional bleaching. To demonstrate the effectiveness of UVA-assisted H_2O_2 bleaching process, two conventional bleaching processes, *i.e.* Pad-steam bleaching, and cold pad-batch bleaching were carried out for comparisons. A conventional scouring process using 2 g L^{-1} surfactant 1303 at 95 °C for 10 min followed by deionized hot water rinse was performed before bleaching.

Pad-steam bleaching. A bleaching solution containing 30 g L^{-1} H_2O_2 and 10 g L^{-1} sodium hydroxide at pH 12.5 was used for dip-pad-dip-pad process. The fabric was then subject to a steaming process at 100 °C for 30 min using a HT-Steamer (Xiamen Rapid, China), rinsed with deionized water, and dried in the open air. Such process and the resultant fabric are denoted as ConvPS (iii) and Sc/Bl_{CONV}-PS (D), respectively.

Cold pad-batch bleaching. A similar process was carried out as described above in *Pad-steam bleaching*. Instead of steaming, the fabric was wrapped with film and subject to a batching process at ambient temperature (20 °C) for 24 h. Such process and the resultant fabric are denoted as ConvCPB (iv) and Sc/Bl_{CONV}-CPB (E), respectively.

2.2.3. CCD research. The experimental design and parameter analysis were carried out on the statistical software package Minitab 19 (State Colleague, PA, USA, Trial version). The effects and interactions including H_2O_2 concentration (g L^{-1}), pH value and UV irradiation time (h) on WI were explored through a CCD experiment (Tables 1 and 2). The average of triplicate measurements was reported. The main effects and interactions between factors were determined according to the ANOVA. All the procedures were followed the description in the Section *2.2.1. UVA-assisted H_2O_2 bleaching* (*One-step process*).

2.2.4. Dyeing. The greige fabric (UnTr.), only scoured control sample (Sc), fabrics treated through UV-assisted bleaching (Sc/Bl_{UVA}-II and Sc/Bl_{UVA}-I) and the fabric using conventional Pad-steam bleaching (Sc/Bl_{CONV}-PS) were used for dyeing. The dyeing process was carried out in the horizontal oscillation dyeing machine. One-bath competitive dyeing experiment was designed to evaluate the dyeability of the above-

Table 1 Variables and experimental design levels

	Levels				
Variables	$-\alpha$	−1	0	1	α
X_1: H_2O_2 (g L^{-1})	3.82	12	24	36	44.18
X_2: pH value	6.64	8	10	12	13.36
X_3: time (h)	0.32	1	2	3	3.68

© 2022 The Author(s). Published by the Royal Society of Chemistry

Open Access Article. Published on 25 3 2022. Downloaded on 2024/10/18 9:57:24.
This article is licensed under a Creative Commons Attribution-NonCommercial 3.0 Unported Licence.

Table 2 Composition of various runs, predicted and actual responses

Run	H_2O_2 (g L^{-1})	pH value	Time (h)	WI	
				Predicted	Actual
1	24	10	0.32	65.42	65.12
2	12	8	3	69.46	69.55
3	24	10	2	72.44	72.60
4	12	12	3	71.79	71.66
5	24	6.64	2	70.13	70.26
6	12	12	1	67.81	68.26
7	24	10	2	72.44	73.00
8	24	10	2	72.44	72.80
9	44.18	10	2	73.19	72.90
10	24	10	2	72.44	71.50
11	24	10	3.68	74.76	74.77
12	24	13.36	2	73.40	72.98
13	36	8	1	68.30	68.65
14	12	8	1	64.73	64.50
15	24	10	2	72.44	72.31
16	36	8	3	75.41	75.17
17	36	12	1	69.85	69.97
18	36	12	3	76.21	76.65
19	24	10	2	72.44	72.46
20	3.82	10	2	66.46	66.45

mentioned 5 fabrics under the same dyeing conditions. One gram of each fabric (5 g in total) was immersed in a 200 mL dyeing solution containing 0.5 g L^{-1} reactive dyes. Dyeing process was set at constant temperature of 40 °C for 20 min under continuous shaking. At first 10 min time point, 6 g sodium sulphate was added to enhance the dye uptake. The temperature was raised up to 90 °C at a rate of 5°C min^{-1} and kept constant for 40 min. Then, 2 g sodium carbonate was added at the first 10 min time point for covalent bonding of reactive dyes on cotton fibre. Finally, the dyed fabrics were individually soaped with 1 g L^{-1} neutral detergent at 90 °C for 3 min and rinsed with deionized water for 3 min. In addition, all the fabric treatment conditions were schematically displayed in Fig. 2a.

2.3. Characterizations

2.3.1. Colour features. The whiteness index (WI), apparent colour depth (K/S), lightness (L^*), redness-greenness index (a^*), yellowness-blueness index (b^*), colour saturation (C) and tristimulus values (X,Y,Z) of fabrics were obtained from a Datacolor 400 spectrophotometer (Datacolor, USA) using Illuminant D65 at 10° observing angle. Four-layered fabric was tested and 10 times of each with average values recorded.

Yellowness Index (YI) of the fabric was calculated using eqn (1),

$$YI = 100 \times (1 - 0.847 \times Z/Y) \quad (1)$$

The standard deviation of K/S was calculated representing the colour uniformity of fabric according to eqn (2),

$$\delta = \sqrt{\frac{\sum_{i=1}^{n}\left[(K/S)_{i,\lambda} - \overline{(K/S)_{\lambda}}\right]^2}{n-1}} \quad (2)$$

where $(K/S)_{i,\lambda}$ is the measured value; $(K/S)_{\lambda}$ is the averaged value; n is 10.

2.3.2. Water absorbance. Water absorbency of the fabric was quantified by water drop elapsing time (s) based on AATCC Test Method 79-2010. The wicking property was tested following FZ/T01071-2008 which references ISO 9073-6:2000. Fabric with specification of 250 × 30 mm^2 was vertically held by a stand. The bottom end (15 mm) of fabric was immersed into water. The wicking height (cm) was recorded after 30 min. A larger

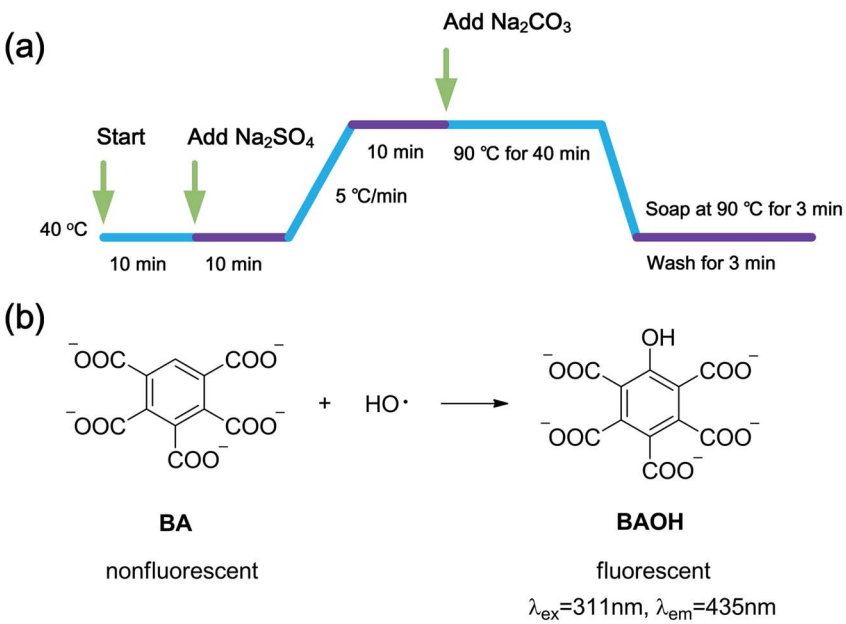

Fig. 2 Schemes for (a) dyeing procedure and (b) fluorescence labelling mechanism.

Open Access Article. Published on 25 3 2022. Downloaded on 2024/10/18 9:57:24.
This article is licensed under a Creative Commons Attribution-NonCommercial 3.0 Unported Licence.

wicking height indicates better water absorbing property. Standardized balancing was taken on all fabrics before measurement.

2.3.3. Tensile property. The breaking strength of the fabric was measured according to ISO 2062 : 2009. On the YG028 universal material testing machine (Wenzhou Fangyuan, China) with a clip distance of 20 cm at a tension speed of 20 cm min^{-1}. Each sample (300 × 50 mm^2) was tested five times both in warp and weft directions to obtain an average value.

2.3.4. SEM and ATR-FTIR. The micro morphology of fabric was observed by SEM (JSM-IT500, JEOL Ltd.) at an acceleration voltage of 20.0 kV. The attenuated total reflectance-Fourier transform infrared (ATR-FTIR) spectra of fabric was obtained on a FTIR-650 spectrometer (Tianjin Gangdong Sci.&Tech. Co., Ltd.) equipped with LA-100 Universal ATR accessory (Lambda Scientific Pty Ltd.).

2.3.5. HO· concentration. The HO· concentration was assessed by fluorescence labeling method which is rapid, sensitive, selective and easy to operate.[31] HO· can be captured by fluorescent probe benzenepentacarboxylic acid (BA), generated single fluorescent products hydroxyl benzenepentacarboxylic acid (HBA) with a maximum emission wavelength at 435 nm (Fig. 2b), which was detected by F-2500 fluorescence spectrophotometer (Hitachi, Japan) with a 10.0 nm band pass slit using an excitation voltage of 700 V. A scan rate of 300 nm min^{-1} was used.

To examine the influence of H_2O_2 dosage on the concentration of HO·, a serials of H_2O_2 solutions at different concentrations (0–1000 μmol L^{-1}) were prepared in the presence of 480 μmol L^{-1} BA. Sodium hydroxide was used to adjust pH value to 10.7. Then, the quartz culture dishes (diameter 10 cm) loaded with 50 mL solutions described above were placed in the lampbox (see Fig. S1†) under the exposure of UVA lamps with a total power of 90 W for 2 h. The fluorescence intensity was measured immediately at the end of the treatment. Fabric and penetrating surfactant were not involved to eliminate their impacts on the accuracy of measurement.

To further examine the effect of UVA irradiation and processing time on the HO· concentration during bleaching process, a simulated bleaching solution containing 480 μmol L^{-1} BA and 400 μmol L^{-1} H_2O_2 at a pH value of 10.7 was prepared. Then, the UVA irradiation was processed for different duration (1–8 h). The control experiment was carried out under the same conditions including solution composition and temperature, only without UVA irradiation. To clarify the effect of HO· on WI, dimethyl sulphoxide (DMSO) was used to scavenge HO·.[19,23] The fabrics were treated according to *One-step process* section and 0–15 mL DMSO was added into the bleaching solution.

2.4. Estimation of energy and water consumption

The energy and water consumptions of three representative bleaching processes, (i) conventional bath scouring/bleaching (Q_{Conv}), (ii) conventional pad-steam scouring/bleaching ($Q_{Sc/BlCONV\text{-}PS}$) and (iii) one-step UVA-assisted bleaching ($Q_{Sc/BlUVA\text{-}I}$), are estimated and compared. More details about the calculation are described in the results and discussion section.

3. Results and discussion

3.1. Bleaching/scouring efficacy

The bleaching and scouring efficacy of different processes is explored through the comparison of the colour feature reflected by WI/YI and *L*/*b* values and water absorbing property of treated fabrics, respectively. Lower YI and *b* values and higher WI and *L* values indicate whiter appearance of fabric due to the higher bleaching efficiency. As seen in Table 3, all the four bleaching processes greatly improve the WI and *L* of fabrics compared with those without treatment and scoured only. In general, the established UVA-assisted bleaching process enables 40% WI enhancement over untreated fabric, which verifies the feasibility of our proposed strategy. Therein, Sc/Bl_{UVA}-II displays a highest WI of 74.55 (42.72% higher than untreated fabric) and lowest YI of 16.63 (34.26% lower than untreated fabric) among the samples. Sc/Bl_{UVA}-I also achieves an equivalent result as Sc/Bl_{UVA}-II, indicating the practicability of single-step UVA-assisted scouring and bleaching for sustainable textile pretreatment in near future. Sc/Bl_{CONV}-CPB has the lowest WI improvement due to the slow H_2O_2 decomposition rate and degradation velocity of colour impurity in ambient condition. A higher WI of Sc/Bl_{UVA}-II over that of Sc/Bl_{CONV}-PS reveals the better bleaching function of catalytic UVA than conventional high-temperature steam. The opposite trends of YI/*b* and WI/*L* values affirmed the credibility of measurements. In general, the wicking height of cotton

Table 3 Colour feature and water absorbing property of fabrics treated with different processes[a]

	Colour feature				Water absorbing property	
Sample	WI (Δ%)	YI (Δ%)	*L* (Δ%)	*b* (Δ%)	Wicking height (cm)	Spreading time (s)
Untr.	52.23 ± 0.18	25.30 ± 0.08	84.93 ± 0.11	11.02 ± 0.06	0.5 ± 0.1	>60
Sc.	56.22 ± 0.61 (7.64)	22.76 ± 0.31 (−10.03)	85.27 ± 0.08 (0.40)	9.13 ± 0.21 (−17.17)	12 ± 0.5	5.5 ± 2.31
Sc/$Bl_{Conv\text{-}PS}$	70.83 ± 0.25 (35.60)	18.93 ± 0.20 (−25.19)	92.40 ± 0.16 (8.80)	6.98 ± 0.16 (−36.66)	12.7 ± 0.6	<1
Sc/$Bl_{Conv\text{-}CPB}$	66.83 ± 0.12 (27.94)	20.07 ± 0.15 (−20.67)	90.58 ± 0.22 (6.66)	7.71 ± 0.12 (−30.06)	13.7 ± 0.5	<1
Sc/Bl_{UVA}-II	74.55 ± 0.69 (42.72)	16.63 ± 0.30 (−34.26)	91.59 ± 0.20 (7.84)	5.26 ± 0.21 (−52.25)	13.2 ± 0.6	<1
Sc/Bl_{UVA}-I	73.64 ± 0.26 (40.99)	17.09 ± 0.05 (−32.46)	91.19 ± 0.34 (7.37)	5.59 ± 0.05 (−49.27)	12.7 ± 0.5	10.5 ± 2.38

[a] Untr.: untreated, Sc.: scoured only, Sc/Bl_{CONV}-PS: conventionally scoured and pad-steam bleached, Sc/Bl_{CONV}-CPB: conventionally scoured and cold pad-batch bleached, Sc/Bl_{UVA}-II: two-step ccoured and UVA-assisted bleached, Sc/Bl_{UVA}-I: one-step scoured and UVA-assisted bleached.

© 2022 The Author(s). Published by the Royal Society of Chemistry

Open Access Article. Published on 25 3 2022. Downloaded on 2024/10/18 9:57:24.
This article is licensed under a Creative Commons Attribution-NonCommercial 3.0 Unported Licence.

fabric higher than 10 cm/30 min fulfils the requirement for the following dyeing and finishing processes.[32] The wicking heights of scoured and scoured/bleached fabric are all increased to a desirable level (≥12 cm/30 min) due to the removal of hydrophobic impurities such as wax, pectin and oil. Two steps conventional (Sc/Bl_{CONV}-PS and Sc/Bl_{CONV}-CPB) and UVA-assisted (Sc/Bl_{UVA}-II) processes further decrease the spreading time than scoured only, which indicates the further removal of hydrophobic impurities during bleaching. However, Sc/Bl_{UVA}-I has longer spreading time than scoured only. This is because fully immersion of fabric in heated scouring bath facilitates the removal of hydrophobic impurity from fibre due to the composite actions such as adequate swelling of impurities and fibre, reduction of interaction between fibre and impurities and enhanced emulsification of surfactant, compared with the case under UVA irradiation. In all, the whiteness and water absorbing property of Sc/Bl_{UVA}-I confirms its feasibility in simultaneous scouring and bleaching of fabric. In-depth exploration of Sc/Bl_{UVA}-I is further carried out in the following sections.

A batch of trials on one-step UVA-assisted bleaching is implemented to discuss impact of factors including additives (surfactant, alkaline and oxidant), techniques (UVA irradiation, heating and stacking), conditions (temperature and time) on the WI and wicking height in 30 min of fabric. Apparently, only UVA radiation can hardly enhance the WI and water absorbing ability (Table 4). With the addition of surfactant, WI increases by 8% with an industrially acceptable wicking height of 10 cm,[32] which indicates the contribution of surfactant on the water absorbing ability of fabric. Alkaline could also remove some of the hydrophobic impurities *via* solubilisation action. Significant enhancement of WI up to 31% occurs upon the combination of H_2O_2 and UVA irradiation, which confirms the efficacy of UVA-assisted bleaching even without alkaline. However, the wicking height is only 9.9 cm lower than those with addition of surfactant. Finally, the best sample with high WI improvement (ΔWI: 40.99%) and water absorbing property (WH: 12.7 cm/30 min) is prepared integrating the usage of surfactant, alkaline, H_2O_2, and UVA irradiation. In fact, such bleaching process integrates physical and chemical mechanisms. Physically, surfactant facilitates the penetration of H_2O_2 into the interior of fibre to get contact with colour impurities. From a chemical perspective, the decomposition rate of H_2O_2 is then accelerated by alkaline thus generating a large quantity of perhydroxyl anions (HO_2^-) that attacks the electrophilic centres of the pigment impurity through nucleophilic reaction (see eqn (i)).[33,34] Under UVA irradiation, HO· is generated due to the photo-induced decomposition of H_2O_2 (see eqn (ii)).[23] Meanwhile, HO_2^- as a nucleophilic reagent further reacts with H_2O_2 to produce HO· (see eqn (iii)).[35] Therein, HO_2^- and HO· are both effective oxidative bleaching species in the bleaching system.

$$H_2O_2 \rightarrow H^+ + HO_2^- \ (pH > 11) \quad (i)$$

$$H_2O_2 \rightarrow 2HO\cdot \ (UVA) \quad (ii)$$

$$HO_2^- + H_2O_2 \rightarrow HO\cdot + HO_2\cdot + HO^- \quad (iii)$$

Finally, high concentrations of oxidative species are generated giving rise to the disintegration of the chromophore chemical structure of the pigment impurity. To validate the role of UVA irradiation during bleaching, another two samples were prepared under heating or stacking in replacement of UVA irradiation. The heating temperature is set at 35 °C to inspect the influence of temperature on bleaching without UVA. Results show that heating makes bare contribution to WI enhancement, reconfirming the good compatibility of UVA, H_2O_2 and NaOH to enhance the WI of fabric. This section verifies the concept on the UVA-assisted bleaching. Further optimisation of parameters are carried out and discussed in the next section (3.2. Modelling and ANOVA).

3.2. Modelling and ANOVA

Based on mathematical modelling method, an optimal equation that describes the relationship of bleaching conditions and WI is generated, which offers evidence for parameter determination during mass production. To gain understanding of the variables' relationship, response surface methodology is used to analyse the data obtained from fewer trials with higher efficiency than 'one-factor-at-a-time' experiment.[36] As displayed in Table 1, the variables *i.e.* H_2O_2 concentration (3.82–44.18 g L^{-1}),

Table 4 Experimental matrix of one-step UVA-assisted bleaching[a]

Additive			Technique			Condition		Indicator	
Surf. (2 g L^{-1})	NaOH (10 g L^{-1})	H_2O_2 (30 g L^{-1})	UVA (60 W)	Heat	Stack	Temp. (°C)	Time (h)	ΔWI (%)	WH (cm/30 min)
✗	✗	✗	✗	✗	✗	✗	✗	—	0.5 ± 0.1
✗	✗	✗	✓	✗	✗	35	2	1.49	0.5 ± 0.1
✓	✗	✗	✓	✗	✗	35	2	8.04	12 ± 0.6
✗	✓	✗	✓	✗	✗	35	2	4.84	6.5 ± 0.4
✓	✓	✗	✓	✗	✗	35	2	9.67	12.5 ± 0.5
✗	✗	✓	✓	✗	✗	35	2	31.63	9.9 ± 0.4
✓	✓	✓	✓	✗	✗	35	2	40.99	12.7 ± 0.5
✓	✓	✓	✗	✓	✗	35	2	20.45	11.8 ± 0.6
✓	✓	✓	✗	✗	✓	20	2	23.99	12.3 ± 0.4

[a] Surf.: surfactant, Temp.: temperature, WH: wicking height.

Open Access Article. Published on 25 3 2022. Downloaded on 2024/10/18 9:57:24.
This article is licensed under a Creative Commons Attribution-NonCommercial 3.0 Unported Licence.

pH value (6.64–13.36) and irradiation time (0.32–3.68 h) are denoted as α, β and γ, respectively, and accordingly a quadratic mathematical equation is designed as follows,

$$\mathrm{WI} = A + B\alpha + C\beta + D\gamma + E\alpha\beta + F\alpha\gamma + G\beta\gamma + H\alpha^2 + I\beta^2 + J\gamma^2$$

where α, β and γ are variables; A is the constant; B, C and D are the coefficients of linear terms; E, F and G are the coefficients of interactive terms; H, I and J are the coefficients of quadratic terms.

The final equation obtained from modelling is described as follows,

$$\mathrm{WI} = 41.78 + 0.5354 \times \mathrm{H_2O_2} + 2.240 \times \mathrm{pH} + 5.84 \times \mathrm{time} - 0.01596 \times \mathrm{H_2O_2} \times \mathrm{pH} + 0.0494 \times \mathrm{H_2O_2} \times \mathrm{time} - 0.0930 \times \mathrm{pH} \times \mathrm{time} - 0.006419 \times \mathrm{H_2O_2} \times \mathrm{H_2O_2} - 0.0593 \times \mathrm{pH} \times \mathrm{pH} - 0.830 \times \mathrm{time} \times \mathrm{time}$$

The significance of the established model and the corresponding coefficients is evaluated by ANOVA (95% confidence), and p-value, respectively. As seen in Table 5, the model F-value (91.18) confirms the significance of the model. The linear coefficients (B, C and D) and square term coefficients (H and J) are very small ($p < 0.001$) except coefficient I of the pH square term, reveals their significance in influencing the WI of fabric. In terms of the 2-way interactions, only the H_2O_2 × time shows significance. The P-value (0.617) of 'lack-of-fit' is much higher over the threshold (0.05), which demonstrates the insignificance of 'lack of fit'. The predicted R-Sq (97.71%) is very close the adjusted R-Sq (94.77%) revealing the high consistency of the predicted and experimental data. The high R^2 (98.80%) approaching 100% indicates the perfect predictability of the established model, which is reconfirmed by the close distribution of predicted plots along with actual plots in Fig. 3.

Table 5 ANOVA for response surface quadratic model

Source	DF	Adj SS	Adj MS	F-Value	P-Value
Model	9	197.184	21.909	91.18	<0.001
Linear	3	172.586	57.529	239.41	<0.001
H_2O_2	1	54.604	54.604	227.24	<0.001
pH	1	12.874	12.874	53.58	<0.001
Time	1	105.108	105.108	437.41	<0.001
Square	3	20.332	6.777	28.20	<0.001
$H_2O_2 \times H_2O_2$	1	12.314	12.314	51.24	<0.001
pH × pH	1	0.810	0.810	3.37	0.096
Time × time	1	9.923	9.923	41.30	<0.001
2-Way interaction	3	4.266	1.422	5.92	0.014
H_2O_2 × pH	1	1.173	1.173	4.88	0.052
H_2O_2 × time	1	2.816	2.816	11.72	0.007
pH × time	1	0.277	0.277	1.15	0.308
Error	10	2.403	0.240		
Lack-of-fit	5	1.034	0.207	0.75	0.617
Pure error	5	1.369	0.274		
Total	19	199.587			
Model summary	S	R-sq	R-sq(adj)	R-sq(pred)	
	0.490	98.80%	97.71%	94.77%	

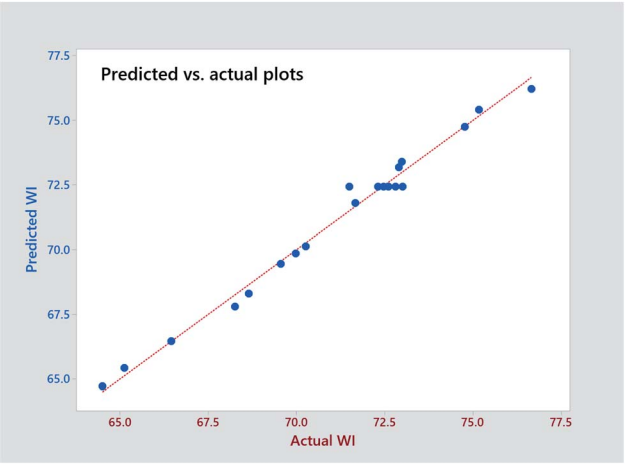

Fig. 3 Graph for actual and predicted plots.

To identify the effect of variables, 2D contour plot for the experimental WI is created based on the quadratic model. As seen in Fig. 4a, the dark green region standing for high WI locates at the upper right corner in the contour plot, which indicates that the higher WI achieves at higher H_2O_2 concentration and pH value. Similar trends are also observed in the contour plots of H_2O_2 concentration *vs.* time (Fig. 4b) and time *vs.* pH (Fig. 4c). Such phenomenon is the consequence of the following factors. Higher concentration of H_2O_2 produces higher quantity of oxidative species that display heavier attack on the chromophore of pigments impurities thus enabling their degradation and decolourization. Higher pH value provided by alkaline accelerates the H_2O_2 decomposition and contributes larger quantity of oxidative species. Apart from chemical reactions, the physical dissolution of hydrophobic impurities and the swelling of cotton fibres for better penetration of H_2O_2 also accounts for such result. Further extending the processing time simultaneously intensifies H_2O_2 decomposition, penetration of oxidative species into fibres, and the oxidation of colour impurities. In general, the result of 2D contour plots suggests that the high WI can be obtained at high levels of H_2O_2 concentration, pH value and time.

Main effect and interaction plots are used to understand the significant extent of variables, and the interactions between each two parameters, respectively.[37] Pareto charts aim to describe the absolute value of the effects. Based on the Pareto chart in Fig. 5a and mean effect plots in Fig. 5b, time is the most noticeable variable, followed by H_2O_2 concentration and pH. The paralleled trend of pH*Time (Fig. 5c) reveals that there is no obvious interactions between them which is consistent with large p-value (0.308) in Table 3. Finally, an optimal bleaching condition (H_2O_2 conc. 42.96 g L^{-1}, pH 10.24 and Time 3.68 h) is obtained, and under which, a theoretical highest WI of 77.19 (47.79% higher than untreated fabric) can be achieved (Fig. 5d).

3.3. Mechanism study

3.3.1. DMSO dosage *vs.* WI. In this study, dimethyl sulphoxide (DMSO) is introduced to the bleaching system to identify

© 2022 The Author(s). Published by the Royal Society of Chemistry

Open Access Article. Published on 25 3 2022. Downloaded on 2024/10/18 9:57:24.
This article is licensed under a Creative Commons Attribution-NonCommercial 3.0 Unported Licence.

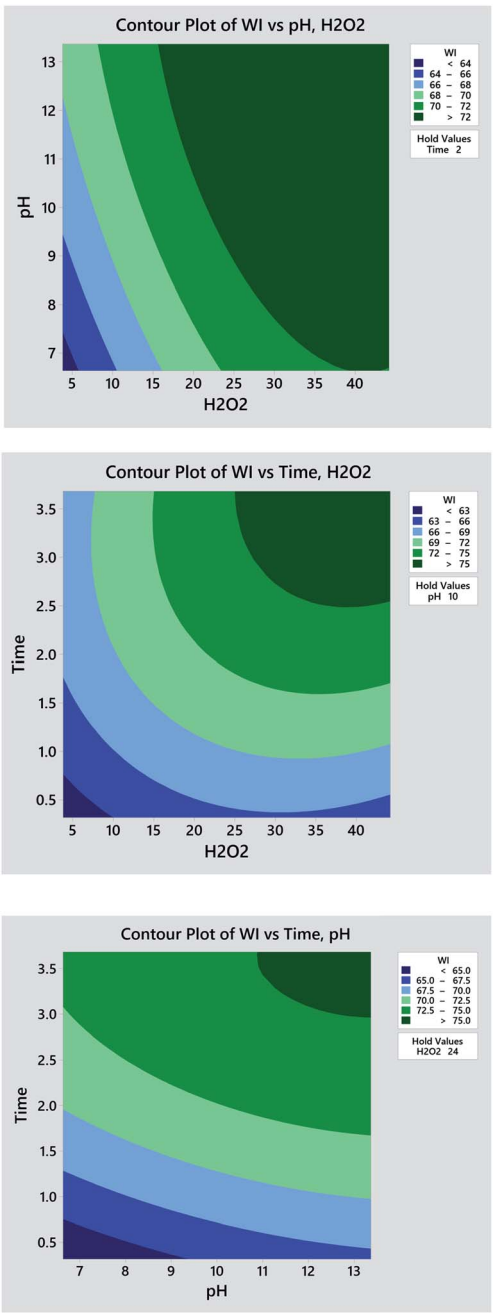

Fig. 4 Contour plots for experimental WI as function of H_2O_2 concentration, pH value and time.

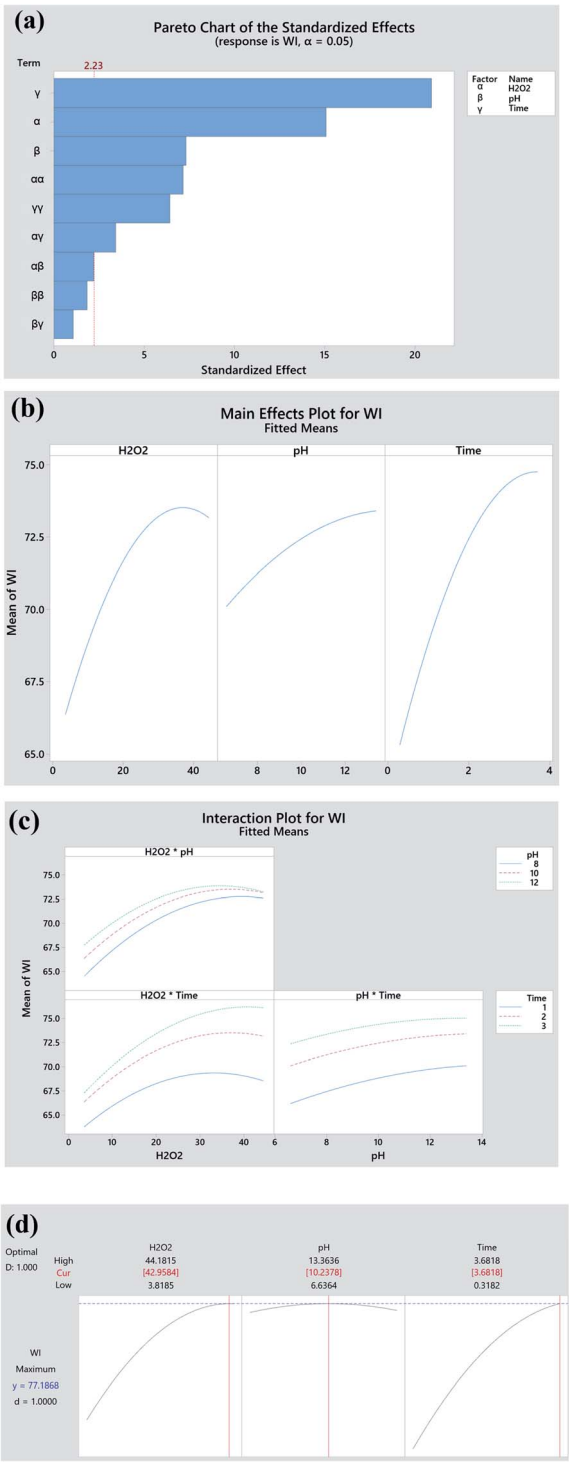

Fig. 5 (a) Pareto chart, (b) main effects, (c) interaction plots, and (d) optimisation.

the impact of HO· concentration on WI under UVA irradiation based on the radical quenching mechanism.[19] As shown in Fig. 6, in UVA-assisted system, the WI decreases almost in a linear downtrend as the increase of DMSO dosage, which confirms the significant role of HO· in the whitening of fabric due to the increased scavenging of HO· by DMSO. Without UVA irradiation, the WI also declined after adding DMSO, indicating the existence of HO· which is probably yielded by the nucleophilic reaction between HO_2^- and H_2O_2 (see eqn (ii)). In all, such result manifests that HO· is the major oxidative species responsible for fabric bleaching. Thus, further investigation is to monitor the HO· concentration in the UVA-assisted bleaching system.

3.3.2. H_2O_2 conc. *vs.* HO· conc.. As discussed in Section 3.2. Modelling and ANOVA, the bleaching effect is highly dependable on the H_2O_2 concentration. In practical textile processing, low H_2O_2 concentration could not impart fabric

Open Access Article. Published on 25 3 2022. Downloaded on 2024/10/18 9:57:24.
This article is licensed under a Creative Commons Attribution-NonCommercial 3.0 Unported Licence.

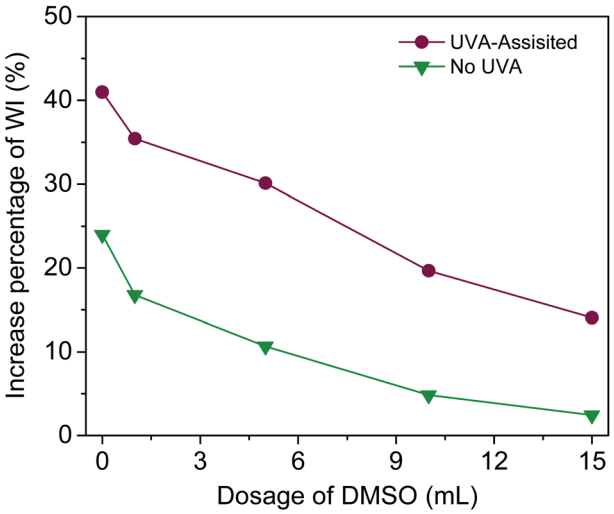

Fig. 6 WI increase percentage as a function of *tert-butanol* concentration. Note: increase percentage of WI of treated fabric is calculated based on the WI of greige fabric.

with desirable whiteness, and overloading of H_2O_2 results in the fibre damage rising from the condensed oxidative HO·. Thus, controlling the usage of H_2O_2 in a reasonable manner is paramount to the whiteness and final quality of fabric. BA is adopted to interact with HO· which is detectable by fluoroscopy. As seen in Fig. 7, the fluorescent intensity at peak wavelength increases with the increase of H_2O_2 concentration in the existence of BA (480 μmol L^{-1}). This is explained by the generation of higher number of HBA at the increasing quantity of HO·. Such results also confirm the feasibility of monitoring the HO· concentration in a bleaching system by using BA.

3.3.3. UVA irradiation time *vs.* HO· conc.. The generation and scavenging of HO· is a dynamic process, in which H_2O_2 continuously decomposes and releases HO· that further reacts with BA and finally form fluorescent HBA.[31] Thus, the reaction time is an important factor to examine the HO· concentration. As illustrated in Fig. 8, a mild increase of fluorescent intensity

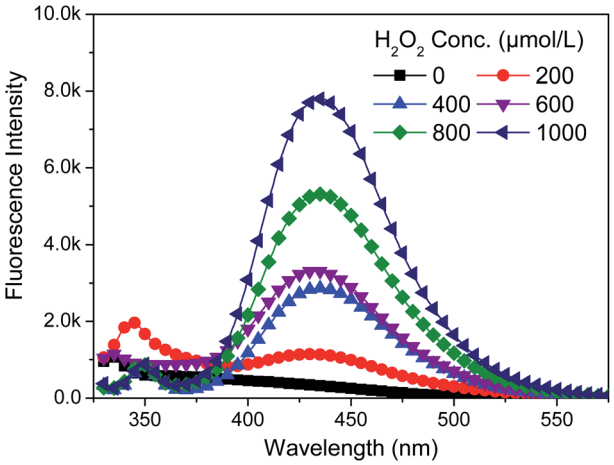

Fig. 7 Fluorensence intensity as a function of H_2O_2 concentration.

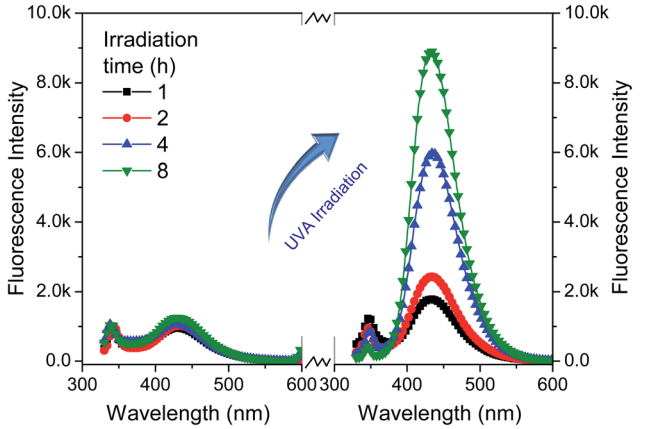

Fig. 8 HO· concentration without (left) and with (right) UVA irradiation as function of time. Note: (H_2O_2 conc.: 400 μmol L^{-1}).

occurs from 900 to 1200 in 8 h without UVA exposure. This reveals that a small quantity of HO· is generated by H_2O_2 due to the low generating rate. Upon the participant of UVA, a dramatic rise of HO· concentration indicated by the florescent intensity of HBA, is observed within 8 h especially during the period of 2–4 h. Such result confirms the catalytic effect of UVA on the decomposition of H_2O_2 to generate HO·, and also visibly describes the catalytic efficiency of UVA on H_2O_2 against time. Considering the time, usage of oxidants and whiteness of fabric, it is reasonable to set the bleaching irradiation duration between 2 to 4 h.

3.4. Dyeing and tensile properties

The colour features and photographs of dyed fabric are displayed in Table 6. Higher apparent colour depth (*K*/*S*) and colour saturation (*C*) indicate a darker colour shade. Apparently, scouring and scouring/bleaching contributes to the darker dyeing effect compared with untreated fabric mainly due to the removal of hydrophobic impurities that impede the dyes migration and penetration towards the fibre during dyeing. One or two steps scouring and UVA-assisted bleaching (Sc/Bl_{UVA}-I and Sc/Bl_{UVA}-II) supports the fabric for a higher dyeing depth (*K*/*S*) than scoured only (Sc.) and conventional two steps (Sc/$Bl_{Conv-PS}$). This is because the established UVA-assisted process achieved a brighter fabric colour (see Table 3) which helps to improve the visual colour depth. The dyeing uniformity of Sc/Bl_{UVA}-I is a little inferior than that of Sc/Bl_{UVA}- II and Sc/Bl_{Conv}-PS, which is mainly attributed to the lower instantaneous water absorbing property of Sc/Bl_{UVA}-I shown in Table 3. However, the difference of dyeing uniformity is almost imperceptible for human eyes, indicating the slightly lower instantaneous water absorbance of Sc/Bl_{UVA}-I does not impact on the dyeing performance. In all, colour feature of the dyed fabric demonstrates the practicability of our established pre-treatment strategy for the subsequent dyeing process.

The mechanical property of bleached fabric is important to the wearing performance of the final textile products. As seen in Table 7, scoured fabric shows a small tensile property decrease than untreated fabric, indicating that heating in the water bath

© 2022 The Author(s). Published by the Royal Society of Chemistry

Open Access Article. Published on 25 3 2022. Downloaded on 2024/10/18 9:57:24.
This article is licensed under a Creative Commons Attribution-NonCommercial 3.0 Unported Licence.

Table 6 Dyeing performance of scoured and bleached fabric[a]

Colour hue	Sample	*K*/*S*	*L*	*a*	*b*	*C*	Uniformity	Photos of dyed fabric
Blue	Untr.	10.46	35.70	−7.60	−20.14	21.53	0.188	
	Sc.	11.20	34.75	−7.29	−20.26	21.53	0.096	
	Sc/Bl_{UVA}-I	11.67	34.38	−7.16	−20.71	21.91	0.133	
	Sc/Bl_{UVA}- II	11.66	34.47	−6.99	−21.11	22.24	0.119	
	Sc/Bl_{Conv}-PS	11.31	34.84	−6.99	−21.14	22.27	0.121	
Yellow	Untr.	6.03	72.86	19.50	65.19	68.05	0.102	
	Sc.	6.51	74.76	22.23	70.14	73.58	0.028	
	Sc/Bl_{UVA}-I	6.83	72.19	20.54	66.99	70.06	0.088	
	Sc/Bl_{UVA}- II	6.81	74.59	22.55	70.94	74.44	0.067	
	Sc/Bl_{Conv}-PS	6.54	74.44	22.36	69.84	73.33	0.044	
Red	Untr.	3.44	60.82	39.06	20.22	43.98	0.039	
	Sc.	3.70	60.22	40.09	20.83	45.18	0.014	
	Sc/Bl_{UVA}-I	4.10	59.01	40.72	21.58	46.09	0.031	
	Sc/Bl_{UVA}- II	4.07	59.11	40.82	21.49	46.13	0.012	
	Sc/Bl_{Conv}-PS	3.86	59.40	40.11	20.97	45.25	0.018	

[a] Untr.: untreated, Sc.: scoured only, Sc/Bl_{CONV}-PS: conventionally scoured and pad-steam bleached, Sc/Bl_{UVA}-II: two-step scoured and UVA-assisted bleached, Sc/Bl_{UVA}-I: one-step scoured and UVA-assisted bleached. Uniformity of colour: standard derivation of *K*/*S*.

Table 7 Tensile property of scoured and bleached fabric[a]

	Warp direction		Weft direction	
Sample	Tensile strength (N)	Elongation (cm)	Tensile strength (N)	Elongation (cm)
Untr.	849.73	2.70	442.86	8.34
Sc.	824.50 (−2.97%)	3.86 (42.96%)	440.86 (−0.45%)	9.07 (8.75%)
Sc/Bl_{UVA}-II	796.06 (−6.32%)	4.15 (53.70%)	404.19 (−8.73%)	10.17 (21.94%)
Sc/Bl_{UVA}-I	803.46 (−5.45%)	4.09 (51.48%)	404.76 (−8.60%)	10.06 (20.62%)
Sc/Bl_{CONV}-PS	806.44 (−5.09%)	4.27 (58.15%)	418.51 (−5.50%)	10.63 (27.46%)

[a] Data in the bracket are the variation percentage over the untreated sample. Abbreviation: Untr.: untreated, Sc.: scoured only, Sc/Bl_{CONV}-PS: conventionally scoured and pad-steam bleached, Sc/Bl_{UVA}-II: two-step scoured and UVA-assisted bleached, Sc/Bl_{UVA}-I: one-step scoured and UVA-assisted bleached.

exert negligible tensile changes. A higher tensile decrease but lower than 10% occurred on the bleached fabrics, which is attributable to the degradation of fiber due to the regional over-oxidation. Fabric has larger elongation in weft direction than in warp direction due to the existence of stretchable spandex fibre. The conventional steam bleaching showed higher strength reservation than UVA-assisted method, which is caused by higher deterioration of cotton fibre in the presence of UVA irradiation and oxidants. Under saturated steam, cotton fibres are wetted and heated which enables the release of the internal stress of macromolecules that finally reduces the fibre breakage due to the concentrated internal stress. Within UV assisted bleaching, UVA/H_2O_2 strategy proposed in this study displays much lower mechanical impact than with UVB and UVC.[24,25]

The similar ATR-FTIR spectra of the untreated and treated fabrics indicate that there is almost no change of functional

Open Access Article. Published on 25 3 2022. Downloaded on 2024/10/18 9:57:24.
This article is licensed under a Creative Commons Attribution-NonCommercial 3.0 Unported Licence.

groups and chemical structure of cotton fibre (Fig. S3†), which is consistent with previous reports.[23,24] Fibre surfaces with and without bleaching are observed by SEM and displayed in Fig. S4.† Impurities in diverse size are observed on the surface of untreated fibre (a–c). One-step UVA-assisted bleaching is able to remove those impurities contributing to a neat fibre surface (d–f).

3.5. Energy and water consumption assessment

The established scoured/UVA-assisted bleaching strategy in this study aims to provide an energy and water-saving alternative to conventional process. The energy consumptions in (i) conventional bath scouring/bleaching (Q_{Conv}), (ii) pad-steam scouring/bleaching ($Q_{Sc/BlCONV\text{-}PS}$) and (iii) one-step UVA-assisted scouring/bleaching ($Q_{Sc/BlUVA\text{-}I}$) processes are estimated and compared in this section. The energy calculation is based on the fabric in 100 m length and 1 m width with the total weight of 29 kg.

(i) For conventional bath scouring/bleaching, Q_{Conv} is the sum of the energy for heating bath solution (Q_1) and fabric (Q_2), and the energy loss by the outer wall of equipment (Q_3),[38]

$$Q_1 = C_1M_1(T_2 - T_1) = 4.186\ \text{kJ kg}^{-1}\ ^\circ\text{C}^{-1} \times 870\ \text{kg} \times (95\text{–}20)\ ^\circ\text{C} = 2.731 \times 10^5\ \text{kJ}$$

$$Q_2 = C_2M_2(T_2 - T_1) = 1.296\ \text{kJ kg}^{-1}\ ^\circ\text{C}^{-1} \times 29\ \text{kg} \times (95\text{–}20)\ ^\circ\text{C} = 2.819 \times 10^3\ \text{kJ}$$

$$Q_3 = \alpha S\Delta TD = 0.02\ \text{kW m}^{-2}\ \text{K}^{-1} \times 13.5\ \text{m}^2 \times 30\ \text{K} \times 1\ \text{h} = 8.1\ \text{kW h} = 2.916 \times 10^4\ \text{kJ}$$

$$Q_{Conv} = Q_1 + Q_2 + Q_3 = 3.051 \times 10^5\ \text{kJ}$$

where, C_1 and C_2 are the specific heat capacity for water and cotton; T_1 and T_2 are the environment and bath temperature; M_1 and M_2 are the weights of bath and fabric (bath ratio of 1 : 30); α is the heat transfer coefficient of air convection; S is the total outer surface area (6 faces of 1.5 m length cubic sealed reservoir) of equipment; ΔT is the temperature difference between environment and outer wall of reservoir; D is the bleaching duration. As the cotton content in fabric (97%) is much higher than spandex (3%), only the specific heat capacity of cotton is involved.

(ii) For pad-steam scouring/bleaching, $Q_{Sc/BlCONV\text{-}PS}$ comprises of energy (Q'_1) for heating fabric, energy (Q'_2) for heating the water content within fabric, energy (Q'_3) for water evaporation from fabric, and energy (Q'_4) loss by the outerwall of steaming setup.[38]

$$Q'_1 = C'_1M'_1(T'_2 - T'_1) = 1.296\ \text{kJ kg}^{-1}\ ^\circ\text{C}^{-1} \times 29\ \text{kg} \times (100\text{–}20)\ ^\circ\text{C} = 3.007 \times 10^3\ \text{kJ}$$

$$Q'_2 = C'_2M'_2(T'_2 - T'_1) = 4.186\ \text{kJ kg}^{-1}\ ^\circ\text{C}^{-1} \times 29\ \text{kg} \times (100\text{–}20)\ ^\circ\text{C} = 9.712 \times 10^3\ \text{kJ}$$

$$Q'_3 = (M'_3/M')H' = (14.5 \times 10^3/18)\ \text{mol} \times 40.668\ \text{kJ mol}^{-1} = 3.276 \times 10^4\ \text{kJ}$$

$$Q'_4 = \alpha'S'\Delta T'D' = 0.02\ \text{kW m}^{-2}\ \text{K}^{-1} \times 67.5\ \text{m}^2 \times 30\ \text{K} \times 1\ \text{h} = 40.5\ \text{kW h} = 1.458 \times 10^5\ \text{kJ}$$

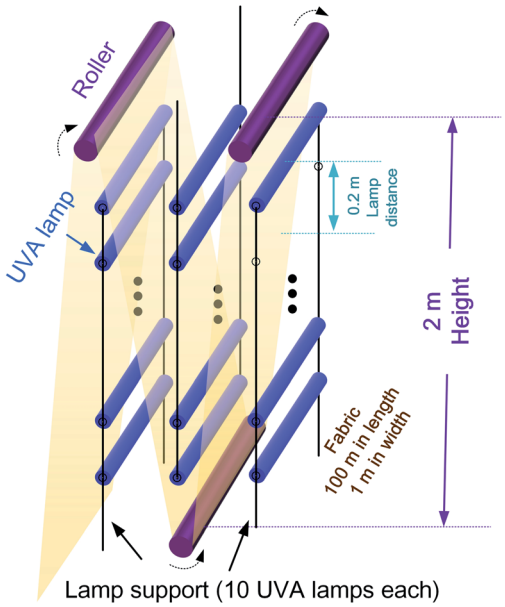

Fig. 9 Proposed continuous UVA-assisted scouring/bleaching process for fabric.

Thus, $Q_{Sc/BlCONV\text{-}PS} = Q'_1 + Q'_2 + Q'_3 + Q'_4 = 1.913 \times 10^5$ kJ

where, C'_1 and C'_2 are the specific heat capacity of cotton and water; T'_1 and T'_2 are the environment and steaming temperature; M'_1 and M'_2 are the weight of fabric and water within fabric (uptake ratio: 100%); M'_3 is the weight of evaporated water from fabric during steaming (evaporation ratio: 50%); M' is molecular weight of water; H' is molar enthalpy of water evaporation; α' is the heat transfer coefficient of air convection; S' is the outerwall area of steaming setup (6 faces of reservoir: 7.5 m in length, 1.5 m in width, 2.5 m in height); ΔT is the temperature difference between environment and outerwall of steaming setup; D is the steaming duration.

(iii) For one-step UVA-assisted scouring/bleaching, $Q_{Sc/BlUVA\text{-}I}$ is merely generated from the consumed electricity for UVA lamp. The continuous manufacturing setup is proposed in Fig. 9. Approx. 500 lamps are required. Based on the experiment Section *2.2.1*, the lamp power of 15 W and irradiation duration of 2 h is adopted for the estimation. Thus, $Q_{Sc/BlUVA\text{-}I} = 500 \times 15\ \text{W} \times 2\ \text{h} = 15\ \text{kW h} = 5.4 \times 10^4$ kJ.

In general, the one-step scoured/UVA-assisted scouring/bleaching process consumes 82.3% and 71.8% less energy than conventional bath and pad-steam scouring/bleaching, respectively. According to the difference of liquor ratio for the conventional bath process (1 : 30) and one-step UVA-assisted process (1 : 15), the water consumption of the former is about twice as much as that of the latter. Therefore, the estimated calculation above confirms the sustainable aspects of one-step scoured/UVA-assisted bleaching strategy in this research.

4. Conclusion

This research introduces an energy/water conservative strategy for one-step scouring/bleaching of cotton/spandex blended

© 2022 The Author(s). Published by the Royal Society of Chemistry

Open Access Article. Published on 25 3 2022. Downloaded on 2024/10/18 9:57:24.
This article is licensed under a Creative Commons Attribution-NonCommercial 3.0 Unported Licence.

fabric using UVA/H_2O_2 system. The efficacy of UVA-assisted bleaching and its mechanism are explored. The significance, interaction and optimisation of parameters are studied *via* mathematical modelling. The dyeing and tensile properties of bleached fabric are analysed. The energy and water consumption are also estimated. Results confirm the potential application of the established one step UVA-assisted scouring/bleaching process for scalable production. The catalytic effect of UVA on bleaching is higher than conventional steaming process. Based on the mathematical modelling, a theoretical highest WI of 77.19 can be obtained using H_2O_2 of 42.96 g L^{-1} at pH of 10.24 for 3.68 h irradiation. In the mechanism study, HO· is proofed as the main oxidative species participating in the UVA-assisted H_2O_2 bleaching. Less than 10% mechanical loss and ideal dyeing property of the fabric which is treated by UVA-assisted method are obtained. More than 70% energy and about 50% water are economised using UVA-assisted bleaching process than conventional process. The UVA-assisted pre-treatment process developed in this study contributes to the sustainable development of textile industry.

Conflicts of interest

There are no conflicts to declare.

Acknowledgements

This work was supported by Opening Project of Key Laboratory of Clean Dyeing and Finishing Technology of Zhejiang Province (QJRZ1902), Opening Project of Jiangsu Engineering Research Center of Textile Dyeing and Printing for Energy Conservation, Discharge Reduction and Cleaner Production (SDGC2101) and Opening Project of Wuhan Research Center of Eco-dyeing & Finishing and Functional Textile (EDFT2021006).

References

1 A. Ahmad, S. H. Mohd-Setapar, C. S. Chuong, A. Khatoon, W. A. Wani, R. Kumar and M. Rafatullah, *RSC Adv.*, 2015, **5**, 30801–30818.
2 M. Shahid, I. Shahid ul and F. Mohammad, *J. Cleaner Prod.*, 2013, **53**, 310–331.
3 I. Shahid ul, M. Shahid and F. Mohammad, *J. Cleaner Prod.*, 2013, **57**, 2–18.
4 N. D. Tissera, R. N. Wijesena and K. M. N. de Silva, *Ultrason. Sonochem.*, 2016, **29**, 270–278.
5 C. Xu, D. Hinks, A. El-Shafei, P. Hauser, M. Li, M. Ankeny and K. Lee, *J. Fiber Bioeng. Inf.*, 2011, **4**, 209–219.
6 E. S. Abdel-Halim, *Carbohydr. Polym.*, 2012, **88**, 1233–1238.
7 P. C. Vandevivere, R. Bianchi and W. Verstraete, *J. Chem. Technol. Biotechnol.*, 1998, **72**, 289–302.
8 R. S. Harane and R. V. Adivarekar, *Text. Cloth. Sustainability*, 2016, **2**, 2.
9 H. Zeng and R.-C. Tang, *J. Text. Inst.*, 2014, **106**, 807–813.
10 Y. Zhou, G. Zheng, J. Zhang, Q. Wang, M. Zhou, Y. Yu and P. Wang, *Cellulose*, 2021, **28**, 8129–8138.
11 K. Liu, X. Zhang and K. Yan, *Carbohydr. Polym.*, 2018, **188**, 221–227.
12 X. Luo, D. Shao, X. Wang, C. Xu and W. Gao, *Cellulose*, 2020, **27**, 5367–5376.
13 S. Wang, S. Li, Q. Zhu and C. Q. Yang, *Ind. Eng. Chem. Res.*, 2014, **53**, 9985–9991.
14 K. Liu, K. Yan and G. Sun, *Cellulose*, 2019, **26**, 2743–2757.
15 S. K. Bhikari Charan Panda, K. Sen and S. Mukhopadhyay, *J. Cleaner Prod.*, 2021, 129725, DOI: 10.1016/j.jclepro.2021.129725.
16 M. İ. Bahtiyari and H. Benli, *Ozone: Sci. Eng.*, 2020, **42**, 450–460.
17 M. Hashem, M. A. Taleb, F. N. El-Shall and K. Haggag, *Carbohydr. Polym.*, 2014, **103**, 385–391.
18 C.-W. Kan, C.-F. Lam, C.-K. Chan and S.-P. Ng, *Carbohydr. Polym.*, 2014, **102**, 167–173.
19 Q. Li, L. Ni, J. Wang, H. Quan and Y. Zhou, *Ultrason. Sonochem.*, 2020, **68**, 105220.
20 H. Ghodbane and O. Hamdaoui, *Chem. Eng. J.*, 2010, **160**, 226–231.
21 T. Zhang and C. H. Huang, *Environ. Sci. Technol.*, 2020, **54**, 7579–7590.
22 B. de Oliveira, L. Moriyama and V. Bagnato, *J. Braz. Chem. Soc.*, 2018, **29**, 1360–1365.
23 N. Wang, P. Tang, C. Zhao, Z. Zhang and G. Sun, *Cellulose*, 2020, **27**, 1071–1083.
24 S. Eren, *Cellulose*, 2018, **25**, 3679–3689.
25 P. Tang and G. Sun, *Carbohydr. Polym.*, 2017, **160**, 153–162.
26 Y. Nie, C. Hu, J. Qu and X. Hu, *J. Hazard. Mater.*, 2008, **154**, 146–152.
27 Y. Nie, X. Sun, M. Wang, X. Tian, C. Yang and C. Dai, *J. Hazard. Mater.*, 2021, **412**, 125259.
28 E. Kattel, M. Trapido and N. Dulova, *Chemosphere*, 2017, **171**, 528–536.
29 R. R. Van Amber, in *Forensic Textile Science*, ed. D. Carr, Woodhead Publishing, 2017, pp. 15–26, DOI: 10.1016/B978-0-08-101872-9.00002-9.
30 S. Tezel and Y. Kavuşturan, *Text. Res. J.*, 2008, **78**, 966–976.
31 F. Si, X. Zhang and K. Yan, *RSC Adv.*, 2014, **4**, 5860.
32 Y.-Z. Lv and X. L. Huang, *Dyeing Finish.*, 2005, **11**, 14–17.
33 N. J. Milne, *J. Surfactants Deterg.*, 1998, **1**, 253–261.
34 D. Scarano, A. Zecchina and S. Bordiga, *J. Chem. Soc., Faraday Trans.*, 1993, **89**, 4123.
35 J. Dannacber and W. Schlenker, *Text. Chem. Color.*, 1996, **28**, 24–28.
36 M. Shahid, Y. Zhou, R.-C. Tang, G. Chen and W. A. Wani, *Dyes Pigm.*, 2017, **138**, 30–38.
37 R. Splechtna, M. Elshehaly, D. Gračanin, M. Đuras, K. Bühler and K. Matković, *Vis. Comput.*, 2015, **31**, 1055–1065.
38 H. X. Yu, R. Y. Li, Z. L. Zhang, B. Pei and H. L. Yu, *Energy Eng.*, 2017, (1), 74–78.

© 2022 The Author(s). Published by the Royal Society of Chemistry